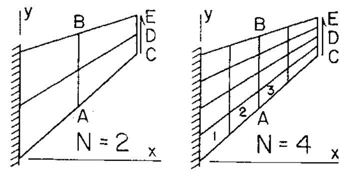

Fig. 1 Arbitrary plane finite-element structure.

$k = j + 1$. Thus, elements of $\mathbf{T}$ for the hybrids may be listed as in Table 1.

Formation of matrix $\mathbf{H}^{-1}$ is trivial for hybrid $H1$. For hybrids $H2$–$H4$, linear and quadratic terms must be integrated to produce $\mathbf{H}$; this is done exactly by Gaussian quadrature using four integration points. Use was made of efficiencies suggested by Irons[3] for integration and manipulation of the form $\mathbf{P}^T\mathbf{N}\mathbf{P}$. Direct formation of $\mathbf{H}$ using properties of plane areas should be faster, but lacks the generality desirable for further extension, e.g., to variable thickness elements.

Formation times for $\mathbf{k}$ are given in Table 2. The trace of $\mathbf{k}$ is given for subsequent reference. Also given in Table 2 is the time required for element stress computation, which consists of reforming $\mathbf{H}^{-1}\mathbf{T}$, postmultiplying by $\mathbf{q}$, premultiplying by $\mathbf{P}$ for each element corner, and printing.

The grade 1 "isoparametric" quadrilateral[3] is a displacement model competitive with the hybrids. Data is given for this model in Table 2. Gaussian quadrature using one point ($I1$) and four points ($I4$) is considered (the latter is exact for a rectangular element). Finally Table 2 lists data for a quadrilateral composed of four constant-strain triangles ($T4$).

Numerical Example and Conclusions

An arbitrary plane structure composed of nonrectangular elements (Fig. 1) was loaded by a uniformly distributed shear τ_{xy} along edge CDE. Finite-element meshes of $N = 1, 2, 4, 8$, and 16 were used.

Vertical deflections of point D for the several meshes and elements are shown in Fig. 2. Validity of the hybrid formulations is confirmed by comparison with displacement models $I1$ and $I4$. Results given by element $T4$ are not shown, as they are practically identical to those given by element $I4$. Excluding $T4$, traces of nonrectangular elements are ranked in the same order seen in Table 2; hence, it appears that the quality of a $\mathbf{k}$ matrix is not directly related to its trace, as has been suggested.[4] One-element structures not shown in Fig. 2 were kinematically unstable.

Stresses plotted in Fig. 3 are averages of stresses along AB in each pair of elements; e.g., along the lower quarter of AB the plotted stress represents $[(\sigma_x \text{ in el. } 2)_{AB} + (\sigma_x \text{ in el. } 3)_{AB}]/2$.

Formulations $H1$ and $I1$ produce identical stiffness matrices, regardless of element shape. Stresses calculated by use of $I1$ are unsatisfactory in a coarse mesh, even though the calculation of stresses from displacements involves no numerical integration; however (as expected[3]) $I1$ is satisfactory in a fine mesh. Hybrid $H1$ seems preferable to both $I1$ and $I4$. Hybrid $H2$ seems preferable to $I4$ in spite of the time disadvantage seen in Table 2. The additional stress modes in $H3$ and $H4$ produce no advantage over $H2$, a conclusion in agreement with remarks of Pian and Tong.[5]

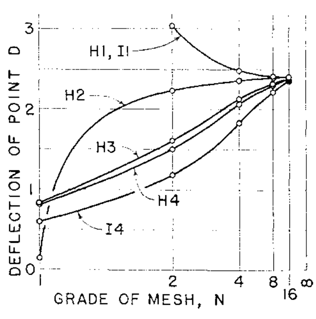

Fig. 2 Vertical deflection of point D in Fig. 1.

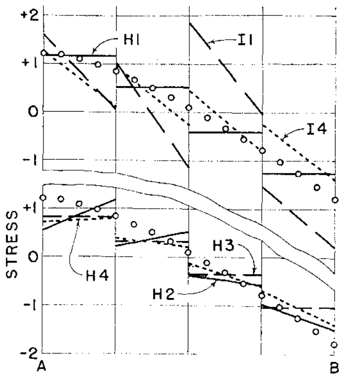

Fig. 3 Stress σ_x along line AB in Fig. 1 for $N = 4$. Circles represent node point averages for $N = 16$ produced by hybrid $H4$.

References

[1] Pian, T. H. H., "Derivation of Element Stiffness Matrices by Assumed Stress Distributions," *AIAA Journal*, Vol. 2, No. 7, July 1964, pp. 1333–1336.

[2] Dungar, R. and Severn, R. T., "Triangular Finite Elements of Variable Thickness and Their Application to Plate and Shell Problems," *Journal of Strain Analysis*, Vol. 4, No. 1, Jan. 1969, pp. 10–21.

[3] Irons, B. M., "Engineering Applications of Numerical Integration in Stiffness Methods," *AIAA Journal*, Vol. 4, No. 11, Nov. 1966, pp. 2035–2037.

[4] Khanna, J., "Criterion for Selecting Stiffness Matrices," *AIAA Journal*, Vol. 3, No. 10, Oct. 1965, p. 1976.

[5] Pian, T. H. H. and Tong, P., "Rationalization in Deriving Element Stiffness Matrix by Assumed Stress Approach," presented at Second Conference on Matrix Methods in Structural Mechanics, Wright-Patterson Air Force Base, Ohio, Oct. 1968.

An Experimental Investigation of the Buckling of Toroidal Shells

B. O. ALMROTH,* L. H. SOBEL,† AND A. R. HUNTER‡

Lockheed Missiles & Space Company, Palo Alto, Calif.

Nomenclature

a = meridional radius of curvature (see Fig. 1)
b = distance between the center of the circular meridian and the axis of revolution (see Fig. 1)
E = Young's modulus
h = thickness of shell
p = uniform hydrostatic pressure loading

THEORETICAL results for the buckling of toroidal shells under uniform external pressure are presented by Sobel and Flügge.[1] These results are in very good agreement with the few available test results. However, these experimental results are for a rather slender torus ($b/a = 8$, see Fig. 1 for notation). Therefore toroidal shells with a smaller value of b/a were manufactured and tested. The dimensions of the tested shells are $b = 5$ in., $a = 2.5$ in, and thickness $h = 0.050$ in. For a meaningful comparison between theory and test, it is important that the test specimen has a reasonably uniform thickness distribution. It was believed that this could best be achieved if the shells are manufactured by casting an epoxy resin material. The toroidal shell was cast in two halves which were later glued together. In this way exces-

Received June 13, 1969. This research was supported by the Independent Research Program of Lockheed Missiles & Space Company.

* Senior Staff Scientist, Aerospace Sciences Laboratory. Member AIAA.

† Research Scientist, Aerospace Sciences Laboratory. Member AIAA.

‡ Research Scientist, Aerospace Sciences Laboratory.

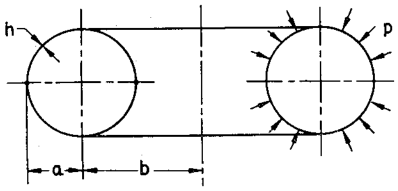

Fig. 1 Notation for a toroidal shell.

sive variations in the thickness were avoided and a high degree of accuracy in the geometry of the shell's middle surface was achieved. To obtain accurate values of the critical pressures for epoxy shells, one must select the material composition in such a way that room temperature creep is minimized. This selection results in a material that has a high modulus and is brittle. Thus when buckling occurs, the shell shatters and it is not possible to observe the development of a buckling pattern. Therefore, in addition to the shells with high modulus, one shell was manufactured from a very ductile material with a low modulus. The epoxy system for the brittle and high-modulus (E = 500,000) material is composed of 100 pbw Bakelite Resin ERL 2774, and 10 pbw Diethanolamine. The low modulus material was obtained through addition of 60 pbw Thiokol LP33 to the composition used for the brittle material. The material components were thoroughly mixed at 100°F. The mold for the half-torus together with the epoxy system was placed in a furnace that was maintained at a temperature of 160°. The epoxy was forced to fill the mold under pressure. The flow rate was held very low in order to minimize entrapment of air. About 1 hr was required to fill the mold. The male mandrel portion of the mold was allowed to free float on the resin such that it lifted when the mold was full. Then the epoxy was allowed to flow over the edges for some time before the free floating mandrel was clamped tight to the female part. After a curing cycle of 24 hr at 160°F the half-shell was removed from the mold. A room temperature curing adhesive was used to bond the two halves of the shell together. The following adhesive composition was selected to match the material properties of the shell: 100 pbw Bakelite Resin ERL 2774, 10 pbw Triethylenetetramine, 3 pbw Aluminum Powder.

Three shells made from the brittle material were tested. External pressure was applied through partial evacuation of the air in the shell. The experimentally determined pressures at failure for the shells are 6.32, 6.60, and 6.64 psi, whereas the theoretical pressure (Ref. 1) based on nominal dimensions is 7.00 psi. After the tests, thickness measurements were made on the shell fragments. It appeared that the thickness was quite uniform but somewhat less than the nominal value of 0.050 in. Thus, the experimental values are somewhat above the theoretical buckling load based on actual dimensions.

One toroidal shell was manufactured from the ductile material. The photographs in Fig. 2 show how the buckling pattern develops for this shell. Figures 2a and 2b, respectively, show the torus before and after application of pressure. From Figs. 2b, it is seen that an axisymmetric deformation pattern has developed. As the load is further increased a nonsymmetrical buckling pattern (see Fig. 2c) is superimposed on the symmetrical pattern. According to theory, the axisymmetric buckling mode is critical for a torus with b/a = 2 and a/h = 50. This buckling pattern appears to be stable (the buckle amplitude grows under increasing load). As a small amplitude symmetric buckling is difficult to detect, it seems possible that the brittle shells really buckled at loads somewhat below those at which the shell shattered. This would tend to explain the somewhat higher values of the experimental buckling pressures.

It can be concluded that for accurately manufactured toroidal shells, such as those tested here, one can expect good agreement between test and theory.

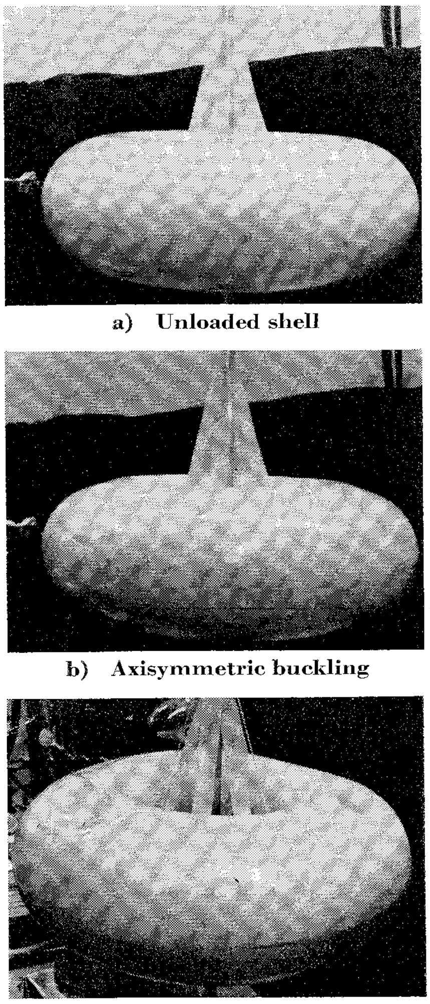

a) Unloaded shell

b) Axisymmetric buckling

c) Nonsymmetric buckling

Fig. 2 Photographs of ductile test specimen.

Reference

[1] Sobel, L. H. and Flügge, W., "Stability of Toroidal Shells under Uniform External Pressure," *AIAA Journal*, Vol. 5, No. 3, March 1967, pp. 425–431.

Optimized Acceleration of Convergence of an Implicit Numerical Solution of the Time-Dependent Navier-Stokes Equations

Joe F. Thompson*
Mississippi State University, State College, Miss.

Nomenclature

ζ = vorticity
ψ = stream function
ω = angular velocity of body
ν = kinematic viscosity
h = cell size
k = time step

Submitted November 15, 1968; presented as Paper 69-185 at the AIAA 7th Aerospace Sciences Meeting, New York, January 20–22, 1969; revision received July 2, 1969. This work wa supported by the U. S. Army Research Office—Durham, Project THEMIS.

* Assistant Professor, Department of Aerophysics and Aerospace Engineering.